Soil Dynamics and Earthquake Engineering 131 (2020) 106012

Contents lists available at ScienceDirect

Soil Dynamics and Earthquake Engineering

journal homepage: http://www.elsevier.com/locate/soildyn

Optimum design of seismic isolation systems using metaheuristic search methods

Ali Erdem Çerçevik [a,*], Özgür Avşar [b], Oğuzhan Hasançebi [c]

[a] Bilecik Seyh Edebali University, Department of Civil Engineering, Bilecik, Turkey
[b] Eskisehir Technical University, Department of Civil Engineering, Eskisehir, Turkey
[c] Middle East Technical University, Department of Civil Engineering, Ankara, Turkey

ARTICLE INFO

Keywords:
Seismic isolated structures
Design optimization
Crow search algorithm (CSA)
Whale optimization algorithm (WOA)
Grey wolf optimizer (GWO)

ABSTRACT

This study addresses the optimum design of seismic isolated structures via metaheuristic search methods. Three recently developed bio-inspired search methods, namely crow search (CSA), whale optimization (WOA) and grey wolf optimizer (GWO), were employed to develop efficient design optimization algorithms for parameter optimization of seismic isolated structures. The developed design optimization algorithms have been applied to optimize a shear frame model with a base isolation system, where the main objective was to obtain isolation system parameters resulting in minimum roof acceleration without exceeding the isolation system displacement limits. The linear isolator system parameters, namely the damping ratio and isolator period, were optimized based on the time history analyses. The optimization procedure was performed for various isolation displacement limits and damping ratio ranges. The results obtained for this isolated structure by the three design optimization algorithms were compared with previously published results in the literature in order to achieve a verification of the developed algorithms. One of the main outcomes of this study is that the high damping ratio does not always guarantee optimum isolation parameters, while an optimum damping ratio is crucial for achieving the minimum roof acceleration.

1. Introduction

The structures are designed to have sufficient rigidity, strength and ductility characteristics to ensure the building safety against the devastating effects of earthquakes in the traditional earthquake-resistant design approach. This approach, which allows certain level of structural and non-structural damages depending on the severity of earthquakes, is not an acceptable design approach for the critical structures that should remain functional during and after an earthquake. Vibration-sensitive equipment housed in strategically critical facilities, such as hospitals, laboratories, air traffic control centers, fire stations, data collection centers, etc. should be serviceable after severe earthquakes in addition to the fulfillment of life safety performance level. One of the most effective methods recommended for such structures is the seismic isolation. Recently, it is becoming more important to design such critical structures without any interruption during their service. For this purpose, floor accelerations, which are critical for both non-structural components as well as the comfort of the residents, need to be minimized in hospitals and buildings containing acceleration sensitive devices. Use of seismic isolation could be an effective method in protecting such strategically important buildings [1–4].

The main idea of the seismic isolation systems, which are generally placed at the basement and in some cases at various levels of the structure, is to ensure the structural functionality by minimizing the earthquake induced seismic effects. By the introduction of isolation devices at the structure, in addition to the lengthening of the fundamental period of the structure, additional damping is provided to reduce the inter-storey drift ratios (ISDR) and the floor accelerations. As a result, the structural and non-structural damage can be reduced effectively not only to guarantee the life safety but also to satisfy serviceability limit state of the structure. Moreover, with the decrease of the floor accelerations, sensitive devices are protected to ensure that they will be able to remain functional during and after the earthquake [5,6].

The most suitable seismic isolation elements should be designed in order to minimize the destructive earthquake effects. Numerous studies were conducted in the literature to design isolator systems that were best suited to construction conditions and requirements [7–11]. Traditional seismic isolator design is made by trial and error approach, where first a

* Corresponding author.
E-mail addresses: erdem.cercevik@bilecik.edu.tr (A.E. Çerçevik), ozguravsar@eskisehir.edu.tr (Ö. Avşar), oguzhan@metu.edu.tr (O. Hasançebi).

https://doi.org/10.1016/j.soildyn.2019.106012
Received 16 September 2019; Received in revised form 10 November 2019; Accepted 16 December 2019
Available online 23 December 2019

structural analysis is performed with initially estimated values of isolation parameters. Then by observing structural response of the isolation system, the isolation parameter values are adjusted and the structural analysis is repeated under this new set of isolation parameters, and so on. The procedure is recurred until the required criteria are met [12]. Although a trial and error approach could somehow be used for the design of linear isolation systems, apparently this is a typical optimization problem where the most effective isolation elements are determined for minimizing the earthquake induced seismic effects.

Depending on the location of the seismic isolated structure with respect to the seismic sources, the seismic effects on the structure can change considerably. Owing to the elongated vibration period of seismically isolated structures, they are less influenced by the far-fault earthquake ground motions with dominant high-frequency content effective in much shorter periods compared to isolation period. On the other hand, the seismic isolated structure can be exposed to very large isolation displacements under the near-fault earthquake ground motions having long period and high amplitude velocity pulses [13]. Supplemental damping can be considered to be a remedy for limiting the large isolation displacements. In case of far-fault earthquakes however, increased damping can result in higher floor accelerations, which is compatible with the design philosophy of seismically isolated structures. Therefore, selection of the most appropriate isolation system parameters, which limit the isolation displacements and at the same time minimizing the floor accelerations, is considered to be an optimization problem.

Various methods have been proposed in the literature for the design of seismic isolated structures to meet the desired performance. Amongst them is optimization of the isolation system parameters. Plenty of studies have been conducted using different methods, such as Kanai–Tajimi spectrum [14], data mining [15], optimality criteria method [16], constrained optimization [17], artificial neural networks [18], stochastic analysis [19], Bouc-wen model [20] for achieving the optimal parameters of the isolation systems. In addition to such studies, finding the optimum isolation system parameters has been recently attempted using various metaheuristic search algorithms such as genetic algorithms [21–25], harmony search algorithm [13], simulated annealing algorithm [26], etc. In these studies usually, floor accelerations were minimized or cost minimization was considered.

This study aims to investigate the use of crow search algorithm (CSA), whale optimization algorithm (WOA) and grey wolf optimization (GWO) in determining optimum values of isolation parameters in seismic isolated structures. It is important to mention that these three bio-inspired search methods are recent additions to metaheuristic search algorithms. Although GWO has found several applications in the area of structural optimization literature [27,28], the use of WOA and CSA is rather limited and immature [29,30]. Besides, it is to the best knowledge of the authors that none of these techniques have been implemented in the literature for parameter optimization problems of seismic isolated systems.

The optimization algorithms developed with the three metaheuristic search methods have been applied to optimize a shear frame model with a base isolation system under various displacement limits as well as supplemental damping ratio and isolation period intervals by minimizing the peak roof acceleration to peak ground acceleration (PRA/PGA) ratio. Structural analyses of the seismic isolated frame were performed by virtue of SAP2000 software, for which the open application-programming interface (OAPI) was implemented to provide data and interaction between the optimization algorithms and structural analysis software. The optimal results achieved for this problem with three developed optimization algorithms were compared with those given by Nigdeli et al. (2014) to verify and quantify numerical performance of the former. The study reveals that the high damping ratio does not always guarantee optimum isolation parameters, while an optimum damping ratio is crucial for achieving the minimum roof acceleration.

2. Problem formulation for optimization of seismic isolation systems

The parameter optimization problem of seismic isolation systems can be stated as follows. The objective is to find linear isolation parameters of a seismic isolated structure,

$$\overrightarrow{X} = (T_0,\ \xi_0) \tag{1}$$

so as to minimize the peak roof acceleration to peak ground acceleration (PRA/PGA) ratio,

$$f = \frac{PRA}{PGA} \tag{2}$$

while satisfying the following constraint:

$$d_0 \le d_{limit} \tag{3}$$

In Eqs. (1)–(3), $\overrightarrow{X}$ is the design variable vector, T_0 is the isolation period, ξ_0 is the isolation damping ratio, d_0 and d_{limit} represent the calculated isolation displacement and its corresponding limit, respectively.

Equivalent isolation period (T_0) is determined using Eq. (4) assuming a rigid-body superstructure motion,

$$T_0 = 2\pi\sqrt{\frac{M_s}{k_0}} \tag{4}$$

and the isolation damping ratio (ξ_0) is determined by Eq. (5).

$$\xi_0 = \frac{c_0 \cdot T_0}{4 \cdot \pi \cdot M_s} \tag{5}$$

where M_s is the total mass of the structure including the mass of the base, k_0 is the effective stiffness of the isolation system and c_0 is the effective viscous damping constant of the isolation system.

In this study, the constraint violations are handled through an external penalty function approach, where a new (constrained) objective function (f_0) is defined by integrating a penalty function term $(f_{penalty})$ to the unconstrained objective function (f) as formulated by Eq. (6).

$$f_o = \frac{PRA}{PGA} \cdot f_{penalty},\ \text{where}\ f_{penalty} = \left(1 + \kappa_1 \cdot \frac{d_0}{d_{limit}}\right)^{\kappa_2} \tag{6}$$

This way, whenever infeasible designs (solutions) are generated for which the calculated isolation exceed the specified isolation displacement limits, they are seriously penalized to steer the search towards feasible regions of the design space. It is worthwhile to mention that the penalty function term used in the present study was taken from Kaveh and Zakian (2013) [31]. For the constants κ_1 and κ_2 in Eq. (6), the values of 1 and 2 can be used, respectively, as recommended by Kaveh and Zakian (2013) [31].

3. Optimization methods employed

Determination of seismic isolation parameters is usually done by trial and error method in a standard design procedure. Although a trial and error approach could somehow be used for the design of linear isolation systems, apparently this is a typical optimization problem where the most effective isolation elements need to be determined for minimizing the earthquake induced seismic effects.

Recently, a group of optimization methods known as metaheuristic search algorithms have been developed as efficient and robust search methodologies. These are nature inspired methods formed by converting basic principles of natural events into numerical optimization algorithms [32–34]. In this study, three recent metaheuristic search algorithms, namely crow search algorithm (CSA), whale optimization algorithm (WOA) and grey wolf optimizer (GWO), were investigated in

terms of their applicability and success in finding optimum isolation parameters of seismic isolated structures. Brief formulations of these search algorithms are presented in the following subsections.

3.1. Crow search algorithm (CSA)

The crow search algorithm (CSA), developed by Askarzadeh (2016), is an efficient metaheuristic algorithm inspired by the intelligent behaviour of crows in nature. The crows follow each other to obtain better food sources. They also store food for their nutrition in other seasons, which is not a type of behaviour observed in other birds. The crows have strong memories, so that they can easily find the location of the stored food. Finding the hidden food source in different places is not an easy task. If the crows notice another crow in the vicinity where they keep food, they try to deceive other crows by moving to a different location [35].

This behaviour of the crows observed in nature was turned into an optimization algorithm through a mathematical model, where crows are searchers, the environment of crows represents the search space, each location of the environment is a feasible solution, the quality of the food is the objective function and the best food is the global best solution of the problem (Askarzadeh, 2016). CSA has been successfully implemented to solve various optimization problems in the literature, such as feature selection problems [36], fractional optimization problems [37], nonlinear optimization problems [38], and engineering optimization problems [39,40]. The step-wise procedure for the implementation of CSA is described as follows:

Step 1. Initialize problem and adjustable parameters: The optimization problem, decision variables and constraints are defined. Then, appropriate values are assigned to the adjustable parameters of CSA, namely flight length (*fl*), namely flock size (*N*), awareness probability (*AP*) and maximum number of iterations ($t_{\max}$).

Step 2. Initialize position and memory of crows: *N* crows are randomly located in a *d*-dimensional search space. Each crow indicates a solution of the problem and *d* is the number of decision variables. In the present study the decision variables refer to isolation period (T_0) and damping ratio (ξ_0). The memory of each crow is initialized. The position of crow *i* in the environment is determined as a vector using Eq. (7) in each iteration *t*. The crows have no experiences at the first iteration, so it is assumed that they have hidden their foods at their initial locations.

$$\vec{X}_i(t) \text{ where } i = 1, 2, \ldots N, \text{ and } t = 1, 2, \ldots t_{max} \tag{7}$$

Effective stiffness of the isolation system k_0 and effective viscous damping constant c_0 values are calculated using Eqs. (4) and (5) for each crow. Then, the calculated k_0 and c_0 values are sent to SAP2000 for performing time history analyses.

Step 3. Time history analysis in SAP2000: Nonlinear time history analyses are performed with predefined earthquake acceleration records, and the isolation displacement (d_0) and peak roof acceleration (PRA) are determined.

Step 4. Evaluate objective function: PRA is divided by peak ground acceleration (PGA) to calculate the PRA/PGA ratio, and the objective function of each crow is calculated in accordance with Eq. (2).

Step 5. Generate new position: The new position of the crow *i* is determined probabilistically in accordance with crow *j* using Eq. (8),

$$\vec{X}_i(t+1) = \begin{cases} \vec{X}_i(t) + r_i \,.\, fl_i(t) \,.\, \left(\vec{M}_j(t) - \vec{X}_i(t)\right) & \text{if } r_j \geq AP_i(t) \\ \textit{a random position} & \textit{otherwise} \end{cases} \tag{8}$$

where $\vec{X}_i(t+1)$ and $\vec{X}_i(t)$ are the position of the crow *i* at iterations *t+1* and *t*, respectively; $fl_i(t)$ is the flight length of crow *i* at iteration *t*; $\vec{M}_j(t)$ is the best so-far position (memory, or food hiding place) of crow *j* at iteration *t*; r_j and r_j are random numbers sampled according to a uniform distribution between 0 and 1; $AP_i(t)$ is the awareness probability of crow *i* at iteration *t*.

Step 6. Check the feasibility of new positions: The feasibility of the new position of each crow is checked. The crow updates its position if the new position is feasible. On the contrary, if the new position is infeasible, the crow does not change its current position.

Step 7: Evaluate objective function of new positions: The objective function value is computed for the new position of each crow using Eq. (6).

Step 8: Update memory: The crows update their memory as follows:

$$\vec{M}_i(t+1) = \begin{cases} \vec{X}_i(t+1) & \textit{if } f(\vec{X}_i(t+1)) < f(\vec{M}_i(t)) \\ \vec{M}_i(t) & \textit{otherwise} \end{cases} \tag{9}$$

where $f(.)$ indicates the objective function value. It is seen that if the objective function value of the new position of a crow is better than the objective function value of the stored position, the crow updates its memory according to the new position through Eq. (9).

Step 9: Check termination criterion: The steps 4–7 are repeated until the termination criterion has been attained. When the termination criterion is met, the best location of the memory in terms of the objective function value is accepted as the optimum solution of the problem.

3.2. Whale optimization algorithm (WOA)

The whale optimization algorithm (WOA) is a metaheuristic algorithm developed by Mirjalili and Lewis (2016). Humpback whales have a unique hunting technique called air bubble behaviour. In this technique humpback whales start searching the prey randomly. The objectives of all the humpback whales are then checked, in which objective refers to the distance of a humpback whale from the prey. Depending on their objectives, other humpback whales then update their location. Air bubble clouds and columns are created by a whale wrap around the prey. When the humpback whale finds the optimal location of prey, it starts encircling the prey and finally hunts it. The complete process can be collected under three search stages as follows [41]:

Step 1. Encircling the preys: In WOA, as in most optimization methods, the search is initiated from the initial random positions. Then the best positions are determined and the other positions are updated according to the best position. The mathematical model of the wrapping strategy is made with the following equations:

$$\vec{D} = |\vec{C} \,.\, \vec{X}^*(t) - \vec{X}(t)| \tag{10}$$

$$\vec{X}(t+1) = \vec{X}^*(t) - \vec{A} \,.\, \vec{D} \tag{11}$$

$$\vec{A} = 2\vec{a} \,.\, \vec{r} - \vec{a} \tag{12}$$

$$\vec{C} = 2 \,.\, \vec{r} \tag{13}$$

where, $\vec{X}$ is the whale position vector and *t* is the current iteration. $\vec{A}$ and $\vec{C}$ are the coefficient vectors, $\vec{X}^*$ is the historical best location, "| |" is absolute value, $\vec{r}$ is *a* random vector in the range of [0,1] and $\vec{a}$ is linearly decreased from 2 to 0 over the course of iterations.

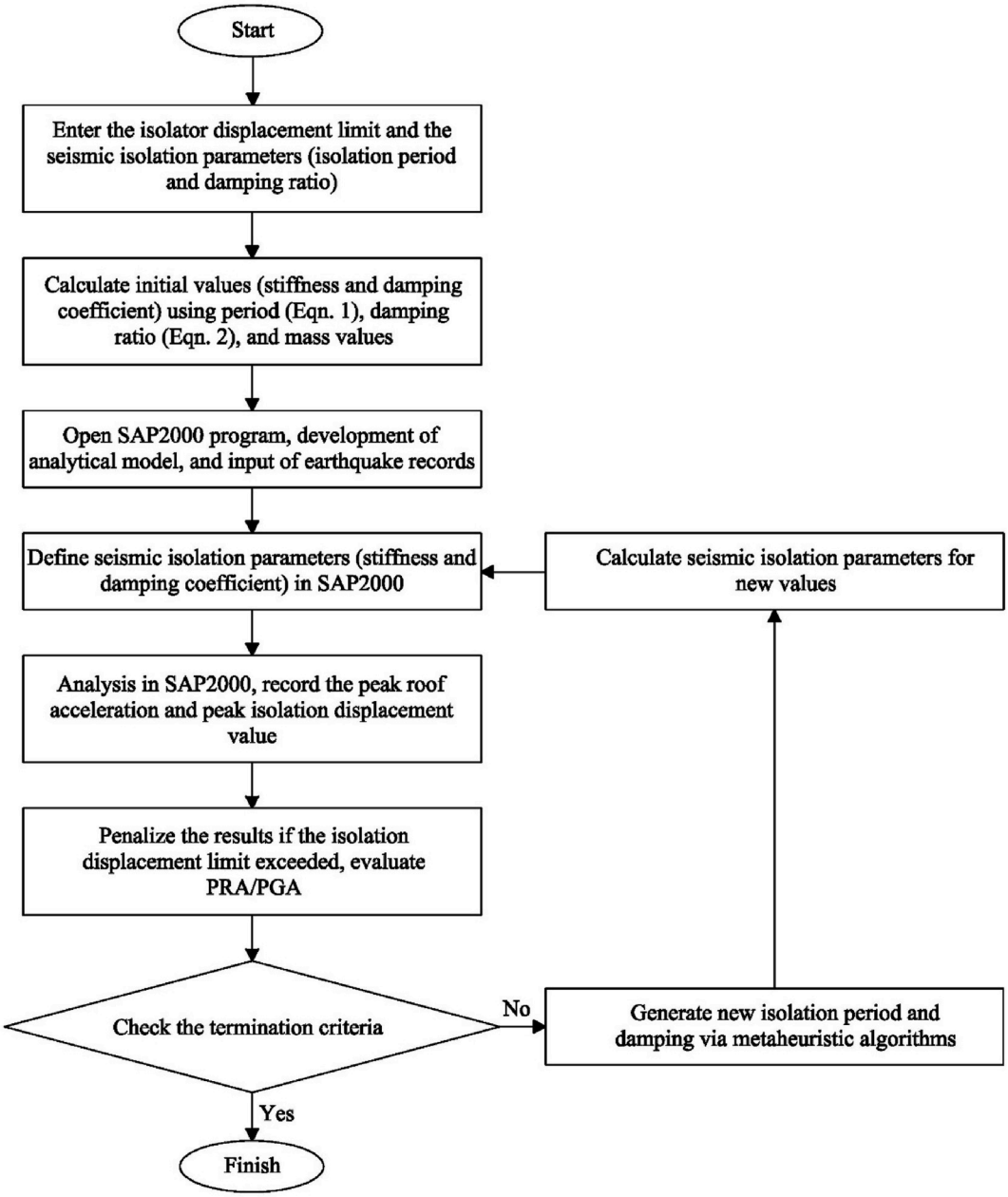

Fig. 1. A general flowchart of the optimization algorithms developed with CSA, WOA and GWO for parameter optimization of seismic isolation systems.

Step 2. Bubble-net attacking method (exploitation phase): The strategy of humpback whales approaching to prey by bubbling is modelled with the following two mechanisms:

1. *Shrinking encircling mechanism:* This behaviour is achieved by decreasing the value of $\vec{a}$ in Eq. (12). It should be noted that $\vec{A}$ is a random value in the interval [−a, a]. Hence, the fluctuation range of $\vec{A}$ is also decreased by $\vec{a}$.
2. *Spiral updating position:* As the humpback whales rise towards their prey, they narrow the spiral and compress their prey into a small area. In the algorithm, the spiral approach or the correct movement to the fish is modelled by the following equations:

$$\vec{X}(t+1) = \vec{D}^{'} . e^{bl} . \cos(2\pi l) + \vec{X}^{*}(t) \tag{14}$$

$$\vec{D}^{'} = | \vec{X}^{*}(t) - \vec{X}(t) | \tag{15}$$

where l is a random number uniformly distributed in the range of [−1,1], b is a constant for defining the shape of the logarithmic spiral, $\vec{D}^{'}$ denotes the distance of the whale i to the prey, and "." is an element-by-element multiplication.

So, the probability of occurrence of the spiral approach update mechanism with the circle collapse movement is 50% in order to model concurrent behaviours during the optimization process. The mathematical model is as follows:

$$\vec{X}(t+1) = \begin{cases} \vec{X}^{*}(t) - \vec{A} . \vec{D} & p < 0.5 \\ \vec{D}^{'} . e^{bl} . \cos(2\pi l) + \vec{X}^{*}(t) & p \geq 0.5 \end{cases} \tag{16}$$

where p is the random number in the range of [0,1].

Step 3. Search for prey (exploration phase): When humpback whales search for fish, they randomly search for the positions of other humpback whales. These movements were modelled as global search except that they collect fish by removing air bubbles in WOA.

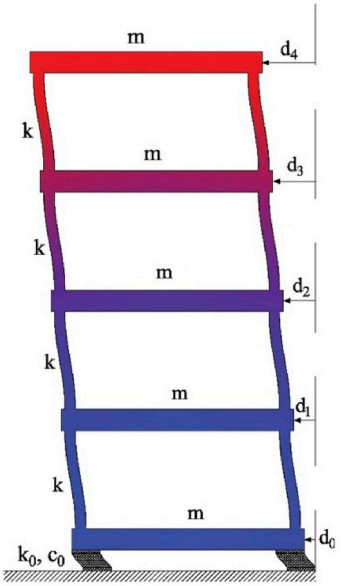

Fig. 2. Schematic representation of the seismically isolated four-storey shear frame and its degrees of freedom [13].

According to this model, global search is the best result in the current iteration, but not random update. WOA can therefore search for the best solution globally in the search space. The mathematical model of this mechanism is made by the following equations:

$$\vec{D} = |\vec{C} \cdot \vec{X}_{rand} - \vec{X}| \tag{17}$$

$$\vec{X}(t+1) = \vec{X}_{rand} - \vec{A}.\vec{D} \tag{18}$$

where $\vec{X}_{rand}$ is a random position vector selected from the current population.

WOA has found some applications in the literature. Kaveh and Ghazaan (2017) employed a modified version of WOA for optimization of skeletal structures. The method has also been applied to different engineering optimization problems such as photovoltaic power systems [42], feature selection [43] and wind speed forecasting [44].

3.3. Grey wolf optimizer (GWO)

Grey Wolf Optimizer (GWO) was introduced by Mirjalili et al. (2014). This algorithm is inspired by unique searching and hunting prey characteristics of grey wolves. Grey wolves usually prefer to live in a pack with a pack size of 5–12 on average. There are four categories in the pack of grey wolves such as α, β, δ, and ω wolves. The leaders in the wolf pack are called alpha and their decisions are dictated to the wolf pack. The second level wolves in the hierarchy are beta wolves. Beta wolfs are lower than alpha wolves that help in the decision making or other pack activities. Omega is the lowest-ranking grey wolf in the pack. If a wolf does not belong to any group mentioned above, it is called delta. GWO optimization consists of five main steps [45]:

Step 1. Social hierarchy: The α, β and δ wolves refer to the first, second, and third best solutions, respectively, while the rest of the candidate solutions are considered as ω.

Step 2. Encircling prey: A grey wolf can update its location around the prey in any random location by using Eqs. 19 and 20.

$$\vec{D} = |\vec{C} \cdot \vec{X}_p(t) - \vec{X}(t)| \tag{19}$$

$$\vec{X}(t+1) = \vec{X}_p(t) - \vec{A}.\vec{D} \tag{20}$$

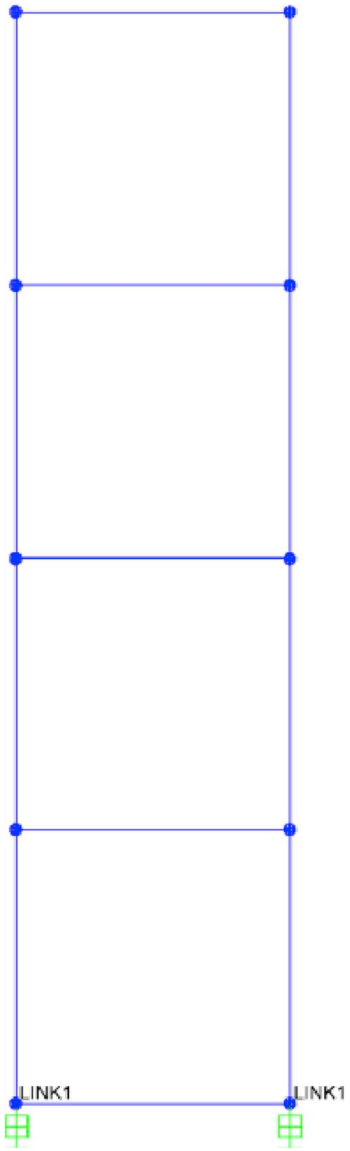

Fig. 3. The model of seismically isolated shear frame developed in SAP2000.

where t indicates the current iteration, $\vec{X}$ indicates the position vector of a grey wolf, $\vec{X}_p$ is the position vector of the prey, $\vec{A}$ and $\vec{C}$ are coefficient vectors, and "| |" is absolute value, and "." an element-by-element multiplication. The coefficients $\vec{A}$ and $\vec{C}$ are computed using Eqs. 21 and 22.

$$\vec{A} = 2\vec{a} \cdot \vec{r}_1 - \vec{a} \tag{21}$$

$$\vec{C} = 2 \cdot \vec{r}_2 \tag{22}$$

where $\vec{r}_1$, $\vec{r}_2$ are random vectors in [0,1].

Step 3. Hunting: The alpha (best candidate solution), beta and delta type grey wolves have superior information about the potential location of prey. Therefore, the first three best solutions are recorded and other search agents are updated for their positions according to the position of the best search agents. The shift of the wolf pack while hunting was modelled mathematically with the following equations:

$$\vec{D}_a = |\vec{C}_1 \cdot \vec{X}_a - \vec{X}| \tag{23}$$

Table 1
Earthquake ground motion records used in the optimization process [51].

Earthquake	Date	Station	Mechanism	Mag (Mw)	Rjb (km)	Component	PGA (g)	PGV (cm/s)	PGD (cm)
Imperial Valley	1940	117 El Centro Array #9	Strike Slip	6.95	6.09	I-ELC180	0.281	30.9	8.66
Kern Country	1952	1095 Taft Lincoln School	Reverse	7.36	38.42	TAFT111	0.180	18.6	9.35
Tabas	1978	9101 Tabas	Reverse	7.35	1.79	TAB-TR	0.861	123.4	93.60
Loma Prieta	1989	16 LGPC	Reverse Oblique	6.93	0	LGP000	0.570	96.1	41.90
Erzincan	1992	95 Erzincan	Strike Slip	6.69	0	ERZ-EW	0.496	78.2	28.04
Northridge	1994	24514 Sylmar OliveView Med FF	Reverse	6.69	1.74	SYL360	0.843	129.4	32.14

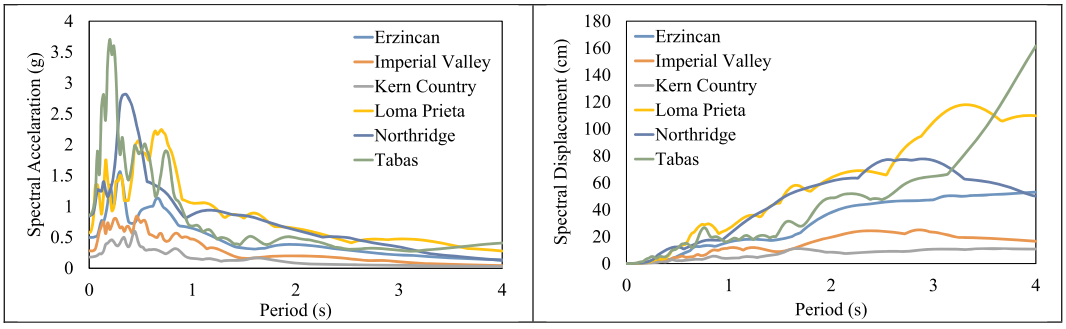

a) Acceleration response spectrum b) Displacement response spectrum

Fig. 4. (a) 5% damped acceleration and (b) displacement response spectra of the selected ground motions.

$$\vec{D}_\beta = |\vec{C}_2 . \vec{X}_\beta - \vec{X}| \quad (24)$$

$$\vec{D}_\delta = |\vec{C}_3 . \vec{X}_\delta - \vec{X}| \quad (25)$$

$$\vec{X}_1 = \vec{X}_a - \vec{A}_1 . (\vec{D}_a) \quad (26)$$

$$\vec{X}_2 = \vec{X}_\beta - \vec{A}_2 . (\vec{D}_\beta) \quad (27)$$

$$\vec{X}_3 = \vec{X}_\delta - \vec{A}_3 . (\vec{D}_\delta) \quad (28)$$

$$\vec{X}(t+1) = \frac{\vec{X}_1 + \vec{X}_2 + \vec{X}_3}{3} \quad (29)$$

Step 4. Attacking prey (exploitation): The grey wolves finish the hunt by attacking the prey when it stops moving. In mathematical model of this behaviour, as the value of $\vec{a}$ decreases, the fluctuation range of $\vec{A}$ also reduces. When $\vec{A}$ has random values in the range [-1, 1], then the search agent's next position will be in any place between its current location and the location of the prey.

Step 5. Search for prey (exploration): Grey wolves usually search according to the location of the alpha, beta, and delta. Each member of the wolf pack is separated from each other to search and attack the prey. In order to mathematically model separation, $\vec{A}$ is utilized with random values greater than 1 or less than −1 to oblige the search agent to separate from the prey. This behaviour of the wolf pack is modelled as GWO's global search.

GWO has been successfully applied to nonlinear engineering problems in the literature, such as scheduling problem [46], robotics and path planning [47] and power engineering problems [48,49], etc. Besides, a modified version of GWO was formulated and implemented for the optimization of truss systems in Kaveh and Zakian (2018) [28].

4. Development of design optimization algorithms

In this study, the design optimization algorithms were developed in MATLAB, where the three metaheuristic search algorithms mentioned in the previous section were integrated with SAP2000 software in order to achieve parameter optimization of seismic isolation systems [50]. This way, structural analyses of the investigated seismic isolated frames were performed by virtue of SAP2000 software, for which the open application-programming interface (OAPI) was implemented to provide data and interaction between the optimization algorithms and structural analysis software.

The isolator stiffness (k_0) and damping coefficient (c_0) values are the two independent variables of the linear properties of the link elements to define linear isolator devices in SAP2000. The variation in the stiffness and damping ratio of the isolation system affects the seismic response of an isolated structure in terms of the roof acceleration and isolator displacement values. The optimum values of k_0 and c_0 are sought for maximum isolator displacement and minimum roof acceleration values by satisfying the specified isolation displacement and damping limits. A general flowchart of the optimization algorithms developed with three metaheuristic search methods (CSA, WOA, GWO) to solve the predefined problem is presented in Fig. 1.

4.1. SAP2000 OAPI implementation

In computer programming, in general, the application programming interface (API) means a sub-application software definition, protocols and tools for creating application software. The SAP2000 open application programming interface enables developers to create, analyse, and design models and automate most of the processes needed to achieve customized analysis and design results. It also provides a way for developers to link SAP2000 with third-party tools, providing a way to exchange two-way model information with other applications. The mechanical properties of the seismic isolator, which is the subject of work with OAPI, can be changed, removed completely or the analysis results can be recalled [50]. These features of OAPI enabled to conduct repetitive solutions with the help of codes developed for the optimization of the seismic isolation parameters.

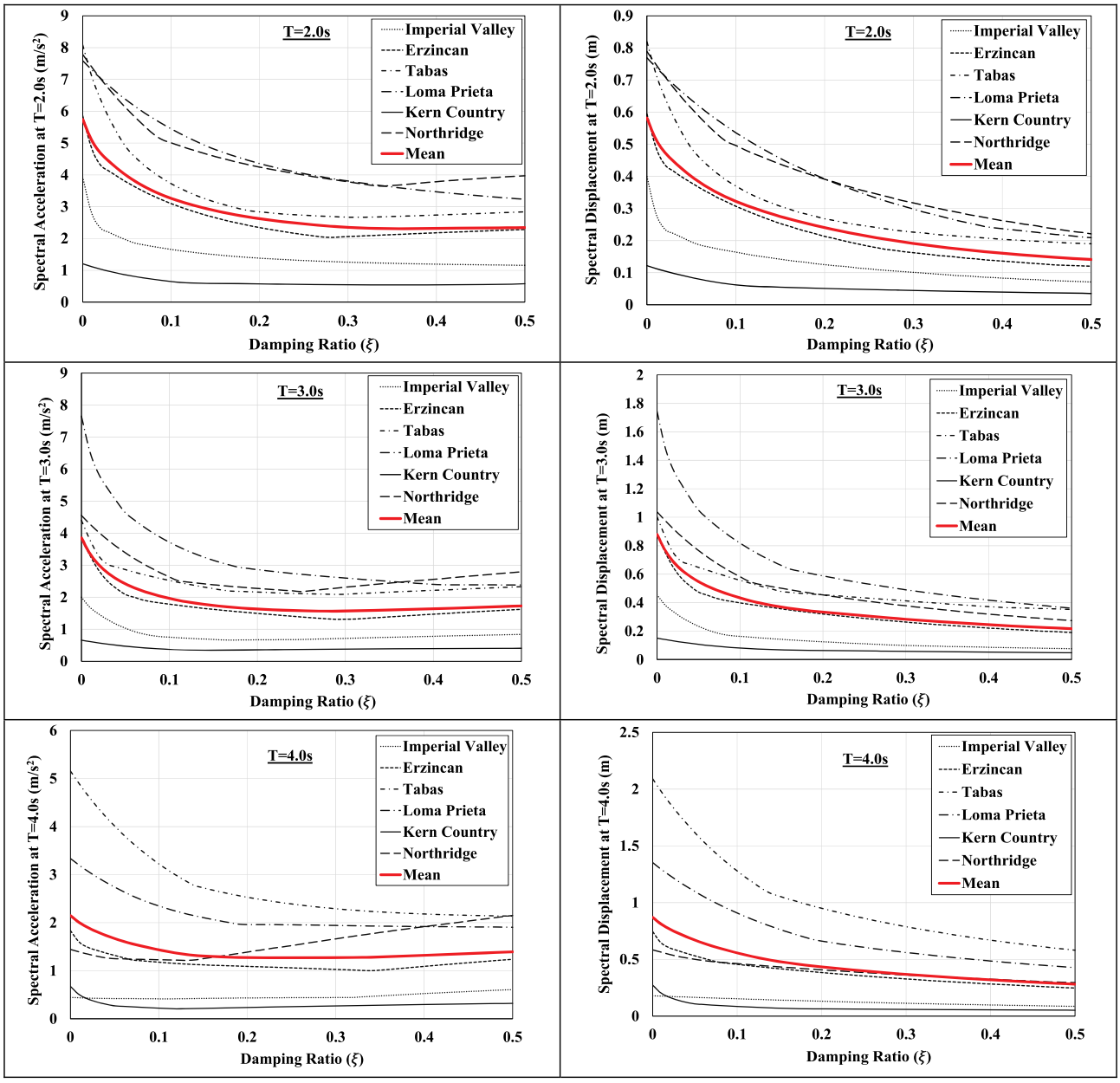

Fig. 5. Variation of spectral acceleration and spectral displacement with damping ratio for various isolation periods.

5. Numerical example

5.1. Test problem

The performances of the optimization algorithms developed in this study with three metaheuristic search methods have been verified and quantified using the four-storey, two-dimensional shear frame shown in Fig. 2. It is important to mention that the optimum seismic isolation parameters of this frame have been previously studied in Nigdeli et al. (2014) using harmony search (HS) method.

5.2. Structural system parameters

The structural system parameters of the shear frame were assigned in accordance with original description of the problem in Nigdeli et al. (2014). Accordingly, story stiffness (k) and floor mass (m) were considered to be the same throughout the shear frame. A floor mass of 1.0 ton was assigned at each floor, which was equally distributed at each floor joint. The stiffness (k) of each storey was adjusted to achieve a fundamental period of 0.4s for the fixed-based analytical model of the shear frame. An additional floor having the same floor mass was defined above the isolator devices. Each floor level was defined to be infinitely rigid, and all the superstructure deformation was dependent on the lateral stiffness of the columns. Accordingly, the structure had only lateral displacement degrees of freedom at each floor level. The viscous damping ratio of the superstructure was assumed to be 5% for all modes.

5.3. Analytical modeling

A two-dimensional analytical model of the seismically isolated shear frame was developed in the SAP2000 structural analysis program (Fig. 3). This model consisted of frame elements for columns and beams, and elastic link elements for isolator devices. In order to define the isolator parameters, elastic link elements were assigned at the base of the analytical model by removing the joint restraints. The elastic properties of the link elements for isolators were defined as the equivalent

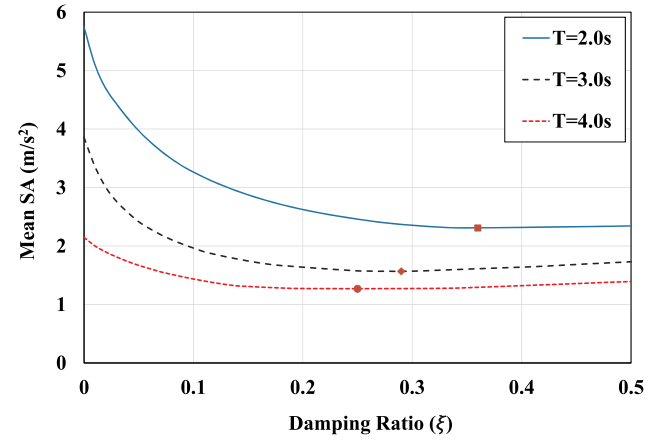

Fig. 6. Mean of the spectral acceleration versus damping ratio for various isolation periods.

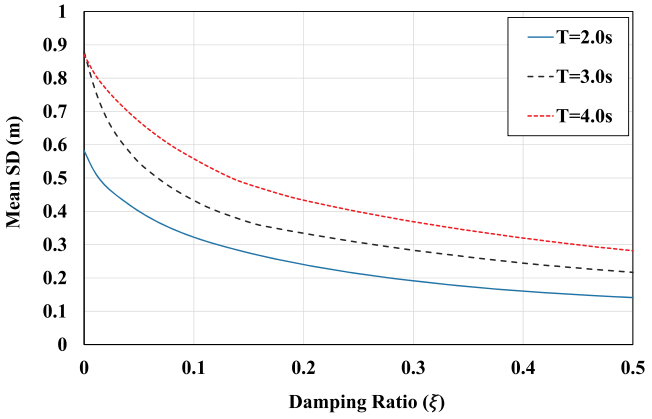

Fig. 7. Mean of the spectral displacement versus damping ratio for various isolation periods.

stiffness and damping coefficients specified in Eqs. (4) and (5), respectively.

5.4. Earthquake ground motion records

A total of six recorded earthquake ground motions were used to implement time history analyses of the analytical model developed. General information and characteristics of the selected ground motion records, which are obtained from PEER ground motion database, including peak ground acceleration (PGA), peak ground velocity (PGV) and peak ground displacement (PGD), are summarized in Table 1. Two of these records are far-fault earthquake records while others are near-fault earthquake records. Among the selected ground motion records, Taft and El Centro ground motion records are considered to be far-fault earthquake records. As presented in Table 1, the seismic intensity measures (PGA, PGV and PGD) of the near-fault ground motions are much higher than the far-fault ground motions. The optimization process for the seismically isolated shear frame was performed by conducting time history analyses with the selected six recorded earthquake ground motions [51].

The 5% damped acceleration and displacement response spectra of the selected six recorded earthquake ground motions are presented in Fig. 4. Spectral ordinates of the far-fault ground motions are smaller than those corresponding to near-fault ground motions.

In addition to the spectral shapes of the selected ground motions, variation of spectral accelerations and displacements with respect to various damping ratios is presented in Fig. 5 for the isolation periods of 2.0s, 3.0s and 4.0s. The investigated period range and the damping ratio range is based on the study of Nigdeli et al. (2014). The mean values of the spectral ordinates of the ground motions with respect to damping ratio are compared in Figs. 6 and 7. It can be observed from these figures that the spectral accelerations decrease, while the spectral displacements increase with the increasing seismic isolation period. This clearly shows that an optimum isolation period needs to be determined for achieving a minimum structural acceleration together with a limited isolation displacement. Although the spectral displacement values reduce considerably with higher damping ratios, the minimum spectral acceleration values are not developed at the maximum considered damping ratios. As shown in Fig. 6, the minimum spectral accelerations occur for the damping ratios that fall in the range of 0.2–0.4 depending on the isolation period. Therefore, Fig. 6 proves that an optimization process needs to be performed to obtain a minimum structural acceleration satisfying with the specified isolation displacement limits.

5.5. Seismic isolation parameters

The two seismic isolation parameters of the shear frame to be optimized refer to the isolation period (T_0) and the isolation damping ratio (ξ_0), as explained in Section 2. The range of isolation period (T_0) for this study was set to vary between 2s and 4s, which is in fact a typical range for many seismically isolated structures [13,52]. On the other hand, three different practical ranges for the isolation system damping ratios were investigated: $0\%<(\xi_0)<30\%$, $0\%<(\xi_0)<40\%$ and $0\%<(\xi_0)<50\%$. In agreement with practical applications, three different cases corresponding to three different peak isolation system displacement limits were also considered as follows: $(d_0)<40$ cm, $(d_0)<50$ cm and $(d_0)<60$ cm. Hence, for each damping ratio and for each displacement limit, analyses were conducted separately, leading to a total of nine different optimization cases.

Table 2
Calculated optimum isolation parameters with CSA, WOA, GWO and comparison with the results of HS.

Case	Isolation system displacement limit (cm)	Isolation system damping ratio range (%)	Optimum isolation system stiffness (kN/m)				Optimum isolation system damping (kN·s/m)			
			HS	Present Study			HS	Present Study		
				CSA	WOA	GWO		CSA	WOA	GWO
1	40	0–30	30.308	28.511	28.453	28.391	7.283	7.121	7.152	7.116
2	40	0–40	22.675	27.686	27.073	26.913	8.458	7.187	7.227	7.243
3	40	0–50	18.590	27.157	26.710	26.494	9.353	7.264	7.361	7.327
4	50	0–30	19.869	17.328	17.374	17.666	5.892	5.511	5.572	5.544
5	50	0–40	16.241	17.059	16.899	16.867	7.105	6.274	6.299	6.198
6	50	0–50	14.493	16.788	16.717	16.717	8.367	6.223	6.248	6.248
7	60	0–30	15.232	15.007	15.087	15.090	5.192	4.964	5.094	5.116
8	60	0–40	13.564	14.317	14.521	14.312	6.505	5.582	5.616	5.627
9	60	0–50	12.500	14.329	14.426	14.227	7.661	5.678	5.544	5.701

Table 3
Percentage difference between the calculated (with CSA, WOA, GWO) optimum isolation parameters and the results of HS.

Case	Isolation system displacement limit (cm)	Isolation system damping ratio range (%)	Optimum isolation system stiffness			Optimum isolation system damping		
			CSA	WOA	GWO	CSA	WOA	GWO
1	40	0–30	−5.9	−6.1	−6.3	−2.2	−1.8	−2.3
2	40	0–40	22.1	19.4	18.7	−15.0	−14.6	−14.4
3	40	0–50	46.1	43.7	42.5	−22.3	−21.3	−21.6
4	50	0–30	−12.8	−12.6	−11.1	−6.5	−5.4	−5.9
5	50	0–40	5.0	4.1	3.9	−11.7	−11.3	−12.8
6	50	0–50	15.8	15.3	15.3	−25.6	−25.3	−25.3
7	60	0–30	−1.5	−1.0	−0.9	−4.4	−1.9	−1.5
8	60	0–40	5.6	7.1	5.5	−14.2	−13.7	−13.5
9	60	0–50	14.6	15.4	13.8	−25.9	−27.6	−25.6

5.6. Optimization parameters

In all the optimization cases, the maximum number of iterations was limited to 100, and population size was set to 25 while running the three optimization algorithms. It was found that the 100 iterations were adequate for the three algorithms to exhibit satisfactory convergence characteristics for the problem of interest. For the CSA algorithm, flight distance and awareness probability were selected as 2 and 0.1, respectively for all the numerical runs.

5.7. Discussion of results

In the following the optimum isolation parameters of the shear frame produced with three metaheuristic search techniques are presented first in nine optimization cases corresponding to different damping ratios and displacement limits. To achieve a level of comparability with other methods, the optimum solutions obtained are also compared to those of Nigdeli et al. (2014), which are referred to as Harmony Search (HS) solutions from this point forward. The convergence characteristics of the three search methods employed are investigated next through the so-called convergence curves. Finally, the discussion is extended to responses of seismically isolated shear frame and determination of dominant earthquake records for the shear frame.

5.7.1. Optimum isolation parameters

The peak PRA/PGA value and isolation displacement from each of the six earthquake records were determined in each iteration and the most unfavourable (maximum isolator displacement or roof acceleration) result was evaluated for each case under the selected earthquake records. For each of the nine cases, three independent runs were performed with each optimization algorithm. The best performance of an algorithm in these runs, i.e. the one leading to the minimum PRA/PGA ratio, was selected as the solution of the algorithm in that particular run.

In Table 2, the optimized stiffness and damping coefficient values obtained by the three algorithms in each of the nine optimization cases are presented and compared with the results of HS. It is seen from Table 2 that the three metaheuristic algorithms have determined lower isolation system stiffness for the damping ratio limit $0\%<(\xi_0)<30\%$ cases, and higher for the $0\%<(\xi_0)<40\%$ and $0\%<(\xi_0)<50\%$ limit cases, in reference to results of HS. On the other side, the damping coefficients obtained by the three algorithms came in the present work out to be consistently lower than those of the reference study for each case considered here. It can be observed that the optimum isolation parameters determined by the three metaheuristic algorithms are indeed very close to each other. The percentage differences between the optimum isolation parameters obtained with CSA, WOA, GWO in the present work and those of the HS are summarized in Table 3.

As can be seen from Table 3, the difference could reach to a maximum value of 46% for the case of 40 cm isolation displacement and $0\%<(\xi_0)<50\%$ damping range. As the damping ratio range increases, the difference between the present work and the reference study become more apparent. For higher isolation damping ratio ranges, the difference between the present work and reference study in terms of optimum isolation system damping gets higher especially for larger isolation system displacement limits.

5.7.2. Convergence curves

The convergence histories displaying the variation of the best design in the most favourable run of the three algorithms (CSA, WSO and GWO) are plotted for each optimization case in Fig. 8. It is noted that the initial values of PRA/PGA differ considerably from one algorithm to another for each case because of the random initialization of the algorithms. It can be seen that the objective functions mostly tend to decrease to an appropriate value after 20–40 generations in each algorithm, indicating that all the three algorithms have very good convergence characteristics. Although there is no remarkable difference in the convergence curves of the algorithms, a slower convergence of CSA is mostly observed as compared to others.

5.7.3. Responses of seismically isolated test problem

The optimum isolation stiffness and damping coefficient values presented in Table 2 were used to model the optimized four-storey seismically isolated shear frame in SAP2000. The time history analyses were performed for the selected six earthquake ground motion records. The resulting PRA/PGA values corresponding to most unfavourable earthquake that caused the maximum analyses results are plotted in Fig. 9 for the nine optimization cases according to three algorithms employed here as well as the HS results.

It can be seen that as the isolation displacement limit increases, the PRA/PGA decreases considerably in each case. The lowest PRA/PGA value was determined for $0\%<(\xi_0)<40\%$ damping and 60 cm isolation displacement limit. When the PRA/PGA results obtained with the optimum isolation parameters found by CSA, WOA and GWO are compared, the difference between the results is negligible. However, HS always obtained higher PRA/PGA values than CSA, WOA and GWO. The difference between the present study and Nigdeli et al. (2014) is apparent especially for the high damping ratio ranges. The reduction in PRA/PGA is not that much significant with the increase in the damping ratio range for the same displacement limit. This observation indicates that the minimum PRA/PGA values do not always occur for the higher damping ratios. This finding is in good agreement with the variation of the mean spectral acceleration of the selected earthquake records with respect to the isolation damping ratio as shown in Fig. 5, which is also supported in the previous studies [53,54]. Furthermore, it is seen in Fig. 10 that the damping ratio of the optimum isolation system by the three metaheuristic algorithms does not reach the upper-bound values of the damping ratio range especially for the higher damping ratios.

Optimum isolator parameters are generally obtained in the range of $\%0<(\xi_0)<\%34$, which is in good agreement with Fig. 5. However, the optimum isolation damping ratio obtained by HS has the tendency to attain the upper-bounds of the damping ratio range. Therefore, there is a considerable difference between the optimum isolation damping ratio obtained by the three algorithms employed here and the HS especially in the higher damping ratio ranges. As a result, increased isolation

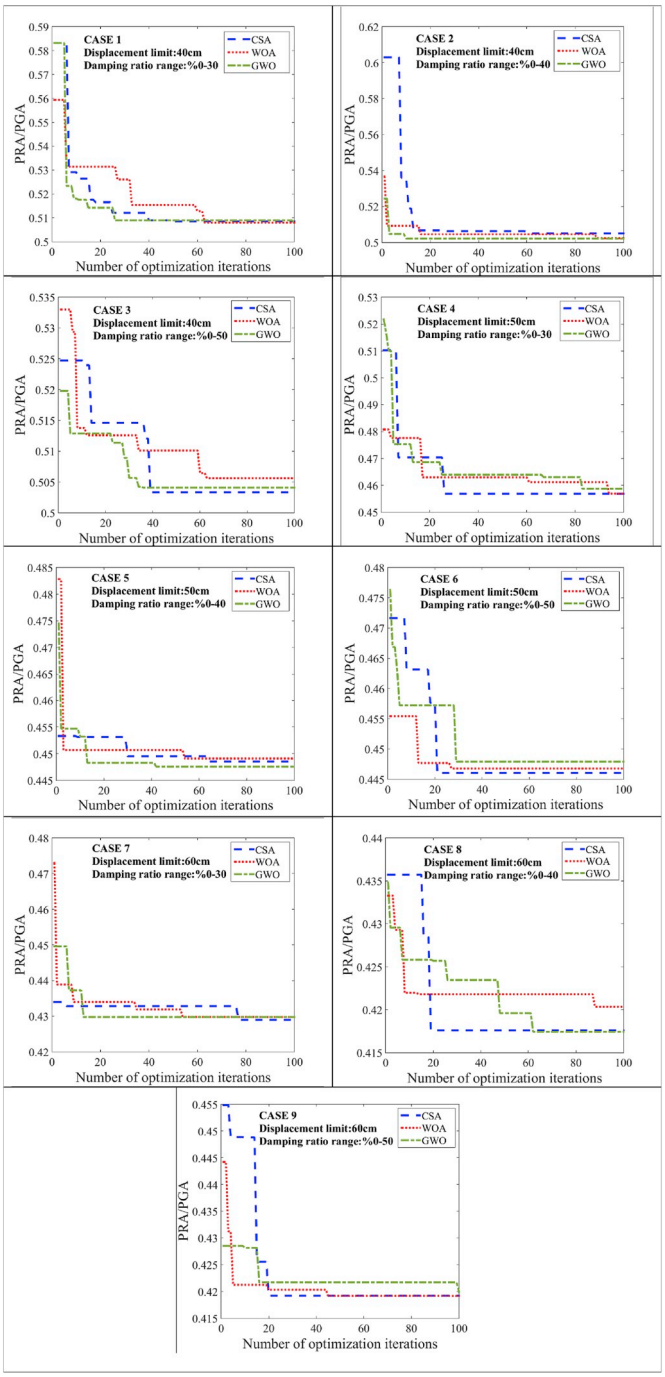

Fig. 8. Comparison of convergence curves for the best runs of CSA, WOA and GWO in the nine optimization cases.

damping by Nigdeli et al. (2014) resulted in an increased level of PRA/PGA as shown in Fig. 8, which is in good agreement with the spectral acceleration trend presented in Fig. 5.

One of the most important consideration in the design of seismically isolated structures is the large amount of isolation displacements due to the increased system flexibility provided by the isolator devices. The isolation displacements should be limited due to the limited space provided around the isolated structure or mostly to ensure the stability of the isolation devise and mechanical and architectural constraints. In this study, the optimization of isolation parameters was carried out in accordance with three different isolation displacement limits. The maximum isolation displacements according to three algorithms employed here as well as the HS are plotted and compared in Fig. 11 for the nine cases.

Fig. 11 reveals that the isolation system displacement converges to the specified displacement limits in all the cases. As the isolation system displacement approaches the limits, the isolation system capacity is used at the maximum level. In most of the cases, the isolation displacement determined according to the optimum isolation parameters by HS remains less than those of the three algorithms employed here. Isolation period values calculated according to the optimum isolation system stiffness and damping coefficient values are presented in Fig. 12.

As shown in Fig. 12, the optimum isolation periods remained between 2s and 4s, which is the isolation period range considered in the optimization process. As expected, the isolation periods converged to the upper limit (4s) as the isolation displacement limits increased. Other than the damping ratio range $0\%<(\xi_0)<30\%$, HS determined higher isolation period compared to the three algorithms employed here. The difference in the isolation period increases as the isolation damping ratio increases.

5.7.4. *Dominant earthquake records for optimum isolation parameters*

One earthquake record amongst the six selected ones seemed to govern the optimum values of isolation parameters for the investigated shear frame. The governing earthquake record changes for each case and for the response parameters of the isolated structure, namely the peak isolation displacement and PRA/PGA ratio. Table 4 indicates that Tabas and Loma Prieta earthquakes are the governing records for all nine cases, yet it may show variation on optimization algorithm level.

Within the scope of this study, it was ensured that the maximum values of the six earthquake records were taken and used in the optimization process. The maximum isolation displacement and the maximum PRA/PGA value can take place under different earthquake records for any case. Loma Prieta and Tabas earthquakes were determined as the most influential earthquake records among the selected six recorded earthquakes (Table 4). Loma Prieta is the dominant earthquake record, generally for smaller isolation displacement limits. Tabas is the dominant earthquake in case of larger isolation displacement limits. It is not possible to make a generalization for the most critical earthquake record that cause the maximum PRA/PGA value, but it can be inferred that the Tabas and Loma Prieta earthquake records are the most influential ones than the others for achieving the maximum structural acceleration. However, the optimization results are quite sensitive to the characteristics of the ground motions because different ground motions can lead to different dynamic responses. Previous studies indicated that the structural responses under seismic effects are related to not only the dynamic characteristics of the structure but also the characteristics of the earthquake ground motions [55,56].

6. Summary and conclusions

In this study, the optimum design of seismic isolation systems was investigated with CSA, WOA and GWO integrated optimization algorithms. A seismically isolated four-storey shear frame model was used for the prototype structure. The shear frame model was developed with SAP2000 and linear time history analyses were performed under the selected six earthquake ground motion records. During the optimization process, the data transfer and interaction between the structural analysis program SAP2000 and the programming language Matlab was provided by open application-programming interface (OAPI).

Within the content of the study, linear isolator system parameters, which are the isolator period and damping ratio, were optimized through the linear time history analyses results by achieving the predefined aim. The optimum isolator parameters for a total of nine different conditions corresponding to three different isolation displacement limits and three different damping ratio limits, were investigated with three metaheuristic algorithms (CSA, WOA and GWO), and the results obtained were compared with the those of Nigdeli et al., 2014, where harmony search method was employed. Based on the results

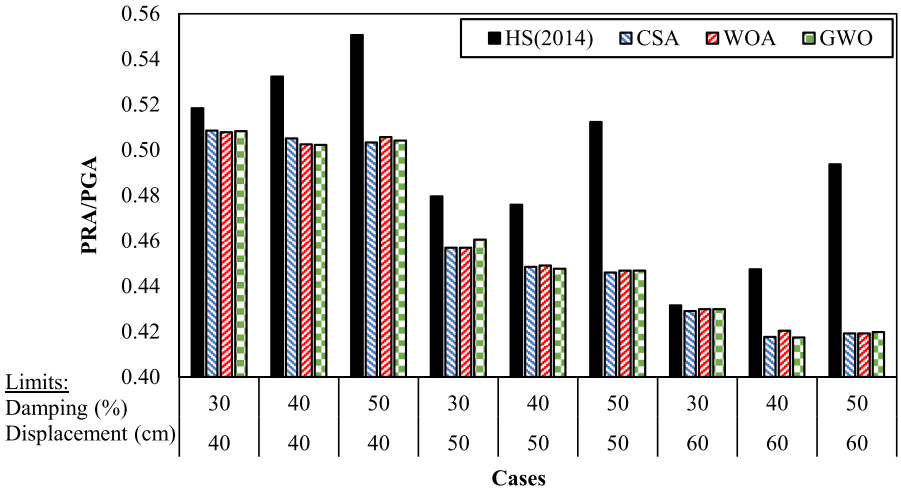

Fig. 9. PRA/PGA ratios evaluated at the optimized designs of CSA, WOA, GWO and HS for the nine optimization cases.

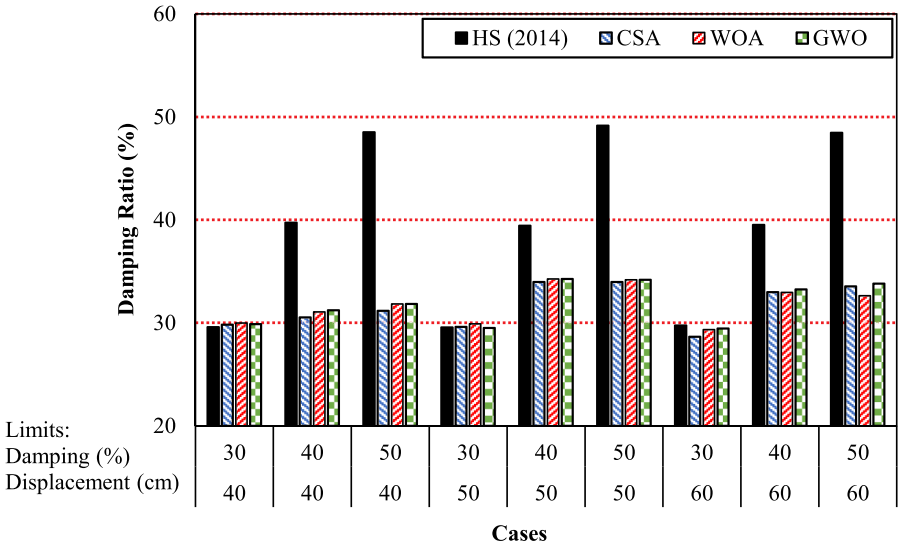

Fig. 10. Damping ratios evaluated at the optimized designs of CSA, WOA, GWO and HS for the nine optimization cases.

obtained in the study, the following conclusions were drawn.

- The optimization study conducted on a seismically isolated 2D structure revealed that the three selected metaheuristic optimization methods can successfully achieve optimum isolation system parameters satisfying the specified design limitations when compared with the optimization results of a previous study.
- The optimum values of isolation parameters in the seismic isolated shear frame considered are mainly controlled by the maximum isolation displacement for larger displacement limits. On the other side, the limiting damping ratio controls the optimum isolation system parameters for low displacement limits.
- Nigdeli et al. (2014), pointed that the minimum PRA/PGA values were obtained at the upper-bounds of the specified damping ratio ranges. However, based on the optimum isolation system parameters obtained by the three metaheuristic algorithms, this study indicated that the minimum PRA/PGA values were achieved at lower damping ratios, instead of upper-bound values. This outcome is compatible with the variation of spectral acceleration with damping ratio at the isolation period range of 2–4s. Accordingly, depending on the isolation period, the peak spectral accelerations occur in the range of 25–35% damping ratio, which is well below the upper-bound values.
- There is no significant variation between the optimum values of the isolation system parameters achieved by the three algorithms (CSA, WOA and GWO). Despite the fact that large variations might occur in the initial PRA/PGA values of the three algorithms due to random initialization of optimization parameters, the objective functions tend to decrease to an appropriate value after 20–40 generations in each algorithm, indicating that all the three algorithms have very good convergence characteristics.
- Among the selected six earthquake records, Tabas and Loma Prieta, which are the near-fault records, are the most influential ones resulting in the most unfavourable seismic response parameters in the optimization process.

Declaration of competing interest

The authors declare that they have no known competing financial interests or personal relationships that could have appeared to influence the work reported in this paper.

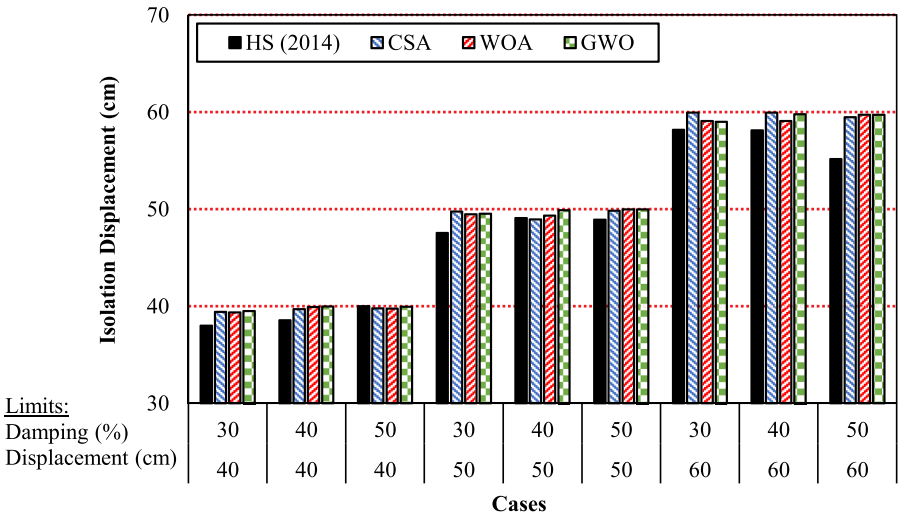

Fig. 11. Isolation displacements evaluated at the optimized designs of CSA, WOA, GWO and HS for the nine optimization cases.

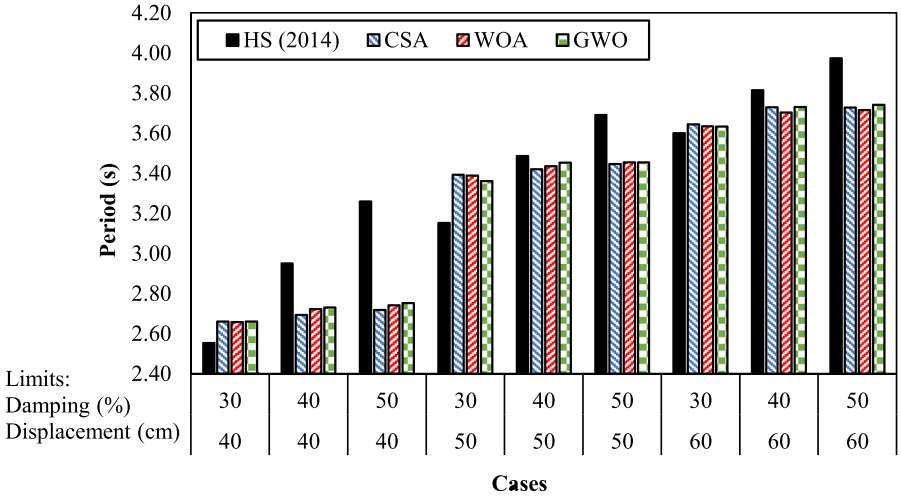

Fig. 12. Isolation period evaluated at the optimized designs of CSA, WOA, GWO and HS for the nine optimization cases.

Table 4
Dominant earthquake records that control the optimum results for 9 different cases and 3 algorithms.

Case	Isolation system displacement limit (cm)	Isolation system damping ratio limit (%)	The maximum displacement			The maximum PRA/PGA		
			CSA	WOA	GWO	CSA	WOA	GWO
1	40	30	Loma Prieta	Loma Prieta	Loma Prieta	Loma Prieta	Loma Prieta	Loma Prieta
2	40	40	Loma Prieta	Loma Prieta	Loma Prieta	Loma Prieta	Loma Prieta	Tabas
3	40	50	Loma Prieta	Loma Prieta	Loma Prieta	Tabas	Tabas	Tabas
4	50	30	Tabas	Loma Prieta	Tabas	Loma Prieta	Loma Prieta	Loma Prieta
5	50	40	Tabas	Tabas	Tabas	Tabas	Tabas	Loma Prieta
6	50	50	Tabas	Tabas	Tabas	Tabas	Tabas	Tabas
7	60	30	Tabas	Tabas	Tabas	Loma Prieta	Loma Prieta	Loma Prieta
8	60	40	Loma Prieta	Tabas	Tabas	Tabas	Loma Prieta	Loma Prieta
9	60	50	Tabas	Tabas	Tabas	Tabas	Loma Prieta	Tabas

References

[1] Iemura H, Taghikhany T, Jain SK. Optimum design of resilient sliding isolation system for seismic protection of equipments. Bull Earthq Eng 2007;5:85–103. https://doi.org/10.1007/s10518-006-9010-5.

[2] Yao GC, Huang WC. Performance of a guideway seismic isolator with magnetic springs for precision machinery. Earthq Eng Struct Dyn 2009;38:181–203. https://doi.org/10.1002/eqe.849.

[3] Tsai CS, Lin YC, Chen WS, Su HC. Tri-directional shaking table tests of vibration sensitive equipment with static dynamics interchangeable-ball pendulum system. Earthq Eng Eng Vib 2010;9:103–12. https://doi.org/10.1007/s11803-010-9009-4.

[4] Alhan C, Şahin F. Protecting vibration-sensitive contents: an investigation of floor accelerations in seismically isolated buildings. Bull Earthq Eng 2011;9:1203–26. https://doi.org/10.1007/s10518-010-9236-0.

[5] Skinner RI, Robinson WH, McVerry GH. Seismic isolation in New Zealand. Nucl Eng Des 1991;127:281–9. https://doi.org/10.1016/0029-5493(91)90052-J.

[6] Naeim F, Kelly J. Design of seismic isolated structures: from theory to practice. John Wiley & Sons.; 1999.

[7] Jangid RS. Optimum frictional elements in sliding isolation systems. Comput Struct 2000;76:651–61. https://doi.org/10.1016/S0045-7949(99)00126-1.

[8] Jangid RS. Optimum lead-rubber isolation bearings for near-fault motions. Eng Struct 2007;29:2503–13. https://doi.org/10.1016/j.engstruct.2006.12.010.

[9] Eltahawy W, Ryan KL, Cesmeci S, Gordaninejad F. Parameters affecting dynamics of three-dimensional seismic isolation. J Earthq Eng 2018. https://doi.org/10.1080/13632469.2018.1537902.

[10] Tubaldi E, Mitoulis SA, Ahmadi H. Comparison of different models for high damping rubber bearings in seismically isolated bridges. Soil Dyn Earthq Eng 2018;104:329–45. https://doi.org/10.1016/j.soildyn.2017.09.017.

[11] Losanno D, Hadad HA, Serino G. Design charts for eurocode-based design of elastomeric seismic isolation systems. Soil Dyn Earthq Eng 2019;119:488–98. https://doi.org/10.1016/j.soildyn.2017.12.017.

[12] Wang Q, Fang H, Zou XK. Application of Micro-GA for optimal cost base isolation design of bridges subject to transient earthquake loads. Struct Multidiscip Optim 2010;41:765–77. https://doi.org/10.1007/s00158-009-0470-5.

[13] Nigdeli SM, Bekdaş G, Alhan C. Optimization of seismic isolation systems via harmony search. Eng Optim 2014;46:1553–69. https://doi.org/10.1080/0305215X.2013.854352.

[14] Baratta A, Corbi I. Optimal design of base-isolators in multi-storey buildings. Comput Struct 2004;82. https://doi.org/10.1016/j.compstruc.2004.03.061. s. 2199–209.

[15] Huang PC, Wan S, Yen JY. A novel method of searching appropriate ranges of base isolation design parameters through entropy-based classification. Struct Control Health Monit 2009;16:385–405. https://doi.org/10.1002/stc.259.

[16] Zou XK. Integrated design optimization of base-isolated concrete buildings under spectrum loading. Struct Multidiscip Optim 2008;36:493–507. https://doi.org/10.1007/s00158-007-0184-5.

[17] Oliveto G, Oliveto ND, Athanasiou A. Constrained optimization for 1-D dynamic and earthquake response analysis of hybrid base-isolation systems. Soil Dyn Earthq Eng 2014;67:44–53. https://doi.org/10.1016/j.soildyn.2014.08.010.

[18] Yucel M, Öncü-Davas S, Nigdeli SM, Bektas G, Sevgen S. Estimating of analysis results for structures with linear base isolation systems using artificial neural network model. IarasOrg 2018;3:50–6.

[19] Fan J, Long X, Zhang Y. Optimum design of lead-rubber bearing system with uncertainty parameters. Struct Eng Mech 2015;56:959–82. https://doi.org/10.12989/sem.2015.56.6.959.

[20] Niola V, Palli G, Strano S, Terzo M. Nonlinear estimation of the Bouc-Wen model with parameter boundaries: application to seismic isolators. Comput Struct 2019;222:1–9. https://doi.org/10.1016/j.compstruc.2019.06.006.

[21] Pourzeynali S, Zarif M. Multi-objective optimization of seismically isolated high-rise building structures using genetic algorithms. J Sound Vib 2008;311:1141–60. https://doi.org/10.1016/j.jsv.2007.10.008.

[22] Charmpis DC, Komodromos P, Phocas MC. Optimized earthquake response of multi-storey buildings with seismic isolation at various elevations. Earthq Eng Struct Dyn 2012;41:2289–310. https://doi.org/10.1002/eqe.2187.

[23] Fallah N, Zamiri G. Multi-objective optimal design of sliding base isolation using genetic algorithm. Sci Iran 2013;20:87–96. https://doi.org/10.1016/j.scient.2012.11.004.

[24] Barakat SA, AlHamaydeh MH, Nassif OM. Optimization of seismic isolation systems with viscous fluid dampers using genetic algorithms. In: COMPDYN 2015 - 5th ECCOMAS thematic conference on computational methods in structural dynamics and earthquake engineering; 2015. https://doi.org/10.7712/120115.3680.1265. s. 4086–95.

[25] Mojolic C, Hulea R, Parv BR. Automatic design optimization tool for passive structural control systems. AIP Conf. Proc. 2017;1863. https://doi.org/10.1063/1.4992719.

[26] Moeindarbari H, Taghikhany T. Novel procedure for reliability-based cost optimization of seismically isolated structures for the protection of critical equipment: a case study using single curved surface sliders. Struct Control Health Monit 2018;25. https://doi.org/10.1002/stc.2054.

[27] Panagant N, Bureerat S. Truss topology, shape and sizing optimization by fully stressed design based on hybrid grey wolf optimization and adaptive differential evolution. Eng Optim 2018;50:1645–61. https://doi.org/10.1080/0305215X.2017.1417400.

[28] Kaveh A, Zakian P. Improved GWO algorithm for optimal design of truss structures. Eng Comput 2018;34:685–707. https://doi.org/10.1007/s00366-017-0567-1.

[29] Kaveh A, Ghazaan I. Enhanced whale optimization algorithm for sizing optimization of skeletal structures. Mech Based Des Struct Mach 2017;45:345–62. https://doi.org/10.1080/15397734.2016.1213639.

[30] Fallah N, Vaez SRH, Mohammadzadeh A. Multi-damage identification of large-scale truss structures using a two-step approach. J. Building Eng. 2018;19:494–505. https://doi.org/10.1016/j.jobe.2018.06.007.

[31] Kaveh A, Zakian P. Optimal design of steel frames under seismic loading using two meta-heuristic algorithms. J Constr Steel Res 2013;82:111–30. https://doi.org/10.1016/j.jcsr.2012.12.003.

[32] Kaveh A. Advances in metaheuristic algorithms for optimal design of structures. second ed. 2016. https://doi.org/10.1007/978-3-319-46173-1.

[33] Kaveh A. Applications of metaheuristic optimization algorithms in civil engineering. 2016. https://doi.org/10.1007/978-3-319-48012-1.

[34] Kaveh A, Bakhshpoori T. Metaheuristics: outlines, MATLAB codes and examples. 2019. https://doi.org/10.1007/978-3-030-04067-3.

[35] Askarzadeh A. A novel metaheuristic method for solving constrained engineering optimization problems: crow search algorithm. Comput Struct 2016;169:1–12. https://doi.org/10.1016/j.compstruc.2016.03.001.

[36] Sayed GI, Hassanien AE, Azar AT. Feature selection via a novel chaotic crow search algorithm. Neural Comput Appl 2019;31:171–88. https://doi.org/10.1007/s00521-017-2988-6.

[37] Rizk-Allah RM, Hassanien AE, Bhattacharyya S. Chaotic crow search algorithm for fractional optimization problems. App. Soft Comp. J. 2018;71:1161–75. https://doi.org/10.1016/j.asoc.2018.03.019.

[38] Jain M, Rani A, Singh V. An improved crow search algorithm for high-dimensional problems. J Intell Fuzzy Syst 2017;33:3597–614. https://doi.org/10.3233/JIFS-17275.

[39] Turgut OE. Crow search based multi-objective optimization of irreversible air refrigerators. Int. J. Intell. Syst. App. Eng. 2018;2:103–12. https://doi.org/10.18201/ijisae.2018642064.

[40] Jamshidi M, Askarzadeh A. Techno-economic analysis and size optimization of an off-grid hybrid photovoltaic, fuel cell and diesel generator system. Sus. Cities. Soc. 2019;44:310–20. https://doi.org/10.1016/j.scs.2018.10.021.

[41] Mirjalili S, Lewis A. The whale optimization algorithm. Adv Eng Software 2016;95:51–67. https://doi.org/10.1016/j.advengsoft.2016.01.008.

[42] Hasanien HM. Performance improvement of photovoltaic power systems using an optimal control strategy based on whale optimization algorithm. Electr Power Syst Res 2018;157:168–76. https://doi.org/10.1016/j.epsr.2017.12.019.

[43] Mafarja M, Mirjalili S. Whale optimization approaches for wrapper feature selection. App. Soft Comp. J. 2018;62:441–53. https://doi.org/10.1016/j.asoc.2017.11.006.

[44] Wang J, Du P, Niu T, Yang W. A novel hybrid system based on a new proposed algorithm—multi-Objective Whale Optimization Algorithm for wind speed forecasting. Appl Energy 2017;208:344–60. https://doi.org/10.1016/j.apenergy.2017.10.031.

[45] Mirjalili S, Mirjalili SM, Lewis A. Grey wolf optimizer. Adv Eng Software 2014;69:46–61. https://doi.org/10.1016/j.advengsoft.2013.12.007.

[46] Lu C, Gao L, Li X, Xiao S. A hybrid multi-objective grey wolf optimizer for dynamic scheduling in a real-world welding industry. Eng Appl Artif Intell 2017;57:61–79. https://doi.org/10.1016/j.engappai.2016.10.013.

[47] Tsai PW, Nguyen TT, Dao TK. Robot path planning optimization based on multiobjective grey wolf optimizer. In: Advances in intelligent systems and computing, vol. 536. Cham: Springer; 2017. https://doi.org/10.1007/978-3-319-48490-7_20. s. 166–73.

[48] Wong LI, Sulaiman MH, Mohamed MR, Hong MS. Grey Wolf Optimizer for solving economic dispatch problems. In: Conference proceeding - 2014 IEEE international conference on power and energy, vol. 2014. PECon; 2014. https://doi.org/10.1109/PECON.2014.7062431. s. 150–4.

[49] Yang B, Yu T, Fang Z, Zhang X, Shu H. Grouped grey wolf optimizer for maximum power point tracking of doubly-fed induction generator based wind turbine. Energy Convers Manag 2016;133:427–43. https://doi.org/10.1016/j.enconman.2016.10.062.

[50] SAP2000. SAP2000 version 20. Structural analysis program: static and dynamic finite element analysis of structures 2019;Version: 1.

[51] PEER. Ground motion database. Shallow crustal earthquakes in active tectonic regimes, NGA-West2. 2019. http://ngawest2.berkeley.edu/.

[52] Pan P, Zamfirescu D, Kashiwa H, Nakayasu N, Nakashima M. Base-isolation design practice in Japan: introduction to the Post-Kobe approach. J Earthq Eng 2008;9:147–71. https://doi.org/10.1080/13632460509350537.

[53] Kelly JM. The role of damping in seismic isolation. Earthq Eng Struct Dyn 1999;28:3–20. https://doi.org/10.1002/(SICI)1096-9845(199901)28:1<3::AID-EQE801>3.0.CO;2-D.

[54] Providakis CP. Effect of LRB isolators and supplemental viscous dampers on seismic isolated buildings under near-fault excitations. Eng Struct 2008;30:1187–98. https://doi.org/10.1016/j.engstruct.2007.07.020.

[55] Trifunac M. How to model amplification of strong earthquake ground motions. Earthq Eng Struct Dyn 1993;22:275.

[56] Fajfar P. Capacity spectrum method based on inelastic demand spectra. Earthq Eng Struct Dyn 1999;28:979–93. https://doi.org/10.1002/(SICI)1096-9845(199909)28:9<979::AID-EQE850>3.0.CO;2-1.